

Excitation and ionization of OCS molecules in strong UV and NIR laser fields

Huijun Shi(师慧军), Yang Liu(刘洋), Tian Sun(孙添), Hang Lv(吕航), and Haifeng Xu(徐海峰)

Citation: Chin. Phys. B, 2024, 33 (**7**): 073301. DOI: 10.1088/1674-1056/ad3035
Journal homepage: http://cpb.iphy.ac.cn; http://iopscience.iop.org/cpb

What follows is a list of articles you may be interested in

Review on non-dipole effects in ionization and harmonic generation of atoms and molecules

Mu-Xue Wang(王慕雪), Si-Ge Chen(陈思格), Hao Liang(梁昊), Liang-You Peng(彭良友)
Chin. Phys. B, 2020, 29 (**1**): 013302. DOI: 10.1088/1674-1056/ab5c10

Effect of laser polarization on strong-field ionization and fragmentation of nitrous oxide molecules

Rui Wang(王瑞), Shi-Wen Zhang(张世文), Yang Liu(刘洋), Tian Sun(孙添), Hang Lv(吕航), Hai-Feng Xu(徐海峰)
Chin. Phys. B, 2019, 28 (**5**): 053301. DOI: 10.1088/1674-1056/28/5/053301

Enhanced ionization of vibrational hot carbon disulfide molecules in strong femtosecond laser fields

Wan-Long Zuo(左万龙), Hang Lv(吕航), Hong-Jing Liang(梁红静), Shi-Min Shan(单石敏), Ri Ma(马日), Bing Yan(闫冰), Hai-Feng Xu(徐海峰)
Chin. Phys. B, 2018, 27 (**6**): 063301. DOI: 10.1088/1674-1056/27/6/063301

Rydberg excitation of neutral nitric oxide molecules instrong UV and near-IR laser fields

Lv Hang (吕航), Zhang Jun-Feng (张军峰), Zuo Wan-Long (左万龙), Xu Hai-Feng (徐海峰), Jin Ming-Xing (金明星), Ding Da-Jun (丁大军)
Chin. Phys. B, 2015, 24 (**6**): 063303. DOI: 10.1088/1674-1056/24/6/063303

Ellipticity-dependent ionization/dissociation of carbon dioxide in strong laser fields

Zhang Jun-Feng (张军峰), Ma Ri (马日), Zuo Wan-Long (左万龙), Lv Hang (吕航), Huang Hong-Wei (黄红卫), Xu Hai-Feng (徐海峰), Jin Ming-Xing (金明星), Ding Da-Jun (丁大军)
Chin. Phys. B, 2015, 24 (**3**): 033302. DOI: 10.1088/1674-1056/24/3/033302

Excitation and ionization of OCS molecules in strong UV and NIR laser fields

Huijun Shi(师慧军), Yang Liu(刘洋), Tian Sun(孙添), Hang Lv(吕航)[†], and Haifeng Xu(徐海峰)[‡]

Institute of Atomic and Molecular Physics, Jilin University, Changchun 130012, *China*

(Received 26 December 2023; revised manuscript received 16 February 2024; accepted manuscript online 5 March 2024)

Rydberg state excitation (RSE) is a highly non-linear physical phenomenon that is induced by the ionization of atoms or molecules in strong femtosecond laser fields. Here we observe that both parent and fragments (S, C, OC) of the triatomic molecule carbonyl sulfide (OCS) can survive strong 800 nm or 400 nm laser fields in high Rydberg states. The dependence of parent and fragment RSE yields on laser intensity and ellipticity is investigated in both laser fields, and the results are compared with those for strong-field ionization. Distinctly different tendencies for laser intensity and ellipticity are observed for fragment RSE compared with the corresponding ions. The mechanisms of RSE and strong-field ionization of OCS molecules in different laser fields are discussed based on the experimental results. Our study sheds some light on the strong-field excitation and ionization of molecules irradiated by femtosecond NIR and UV laser fields.

Keywords: Rydberg state excitation, strong field, carbonyl sulfide, ionization

PACS: 33.80.Rv, 34.80.Gs **DOI:** 10.1088/1674-1056/ad3035

1. Introduction

The interaction of atoms or molecules with femtosecond strong laser fields has attracted lots of experimental and theoretical researches during the past several decades.[1–3] Ionization[4] is viewed as the fundamental process in strong-field physics, and may induce various nonlinear physical phenomena, including non-sequential double/multiple ionization (NSD(M)I),[5,6] high-order above-threshold ionization[7,8] and high-order harmonic generation.[9] Recently, it has been surprising to find, both theoretically and experimentally, that neutral atoms and molecules in Rydberg states can survive strong laser fields.[10,11] Such Rydberg-state excitation (RSE) provides an important complementary aspect to the picture of strong laser atom/molecule interaction, and can be of potential application in neutral particle acceleration[12] and coherent light emission.[13]

Previous studies mainly concerned the strong-field RSE of atoms, with the underlying mechanism being investigated. In different laser fields, the Rydberg state could be populated either by recapturing the low-energy photo-electrons[10,14–16] or by absorbing multi-photons resonantly.[17,18] A distinct oscillation structure in the laser intensity dependence of RSE population has been observed in experimental measurements, and has been well reproduced by the time-dependent Schrödinger equation[19,20] and full quantum-mechanical calculation.[21,22] The oscillation can be attributed to the interference between electronic wave packets liberated in different optical cycles, indicating a quantum effect in strong-field RSE of atoms.

On the other hand, much less is known about molecular RSE in strong laser fields. RSE of the diatomic molecules N_2 and O_2 has been observed in strong 800 nm laser fields and the results have been compared with their companion atoms with similar ionization potential.[23] It has been found that the probability of molecular RSE strongly depends on the structure of the molecular orbitals. Energetic fragment Rydbergs have been observed for diatomic molecules (H_2,[24] D_2,[25] N_2,[26] CO[27]) and dimers (Ar_2,[28] N_2Ar[29]) as well as small triatomic molecules (D_3)[30] in strong laser fields. The kinetic energy releases of these fragment Rydbergs are found to be similar to the corresponding fragment ions. It is indicated that these fragment Rydbergs mainly come from the recapture of low-energy photo-electrons by corresponding fragment ions that are produced by dissociation or Coulomb explosion of parent ions. Nevertheless, molecular RSE induced by strong laser fields, as well as the relation to the strong-field ionization, is far from completely understood. Further investigation on molecular RSE would add more knowledge about strong-field nonlinear dynamic processes.

Carbonyl sulfide (OCS) is important in the global cycling of sulfur and has been discovered in the atmosphere, volcanic gases, ice cores in Antarctica and the interstellar medium. Photo-ionization/dissociation of OCS, which plays a pivotal role in various light-induced chemical and physical processes involving the molecule, has been widely investigated using synchrotron radiation,[31–33] ion impact[34,35] and intense lasers.[36] With regard to strong femtosecond laser pulses, the Coulomb explosion of OCS has been investigated using ion-momentum imaging and the structure of the exploding molecule has been retrieved, the results of which

[†]Corresponding author. E-mail: Lvhang0811@jlu.edu.cn
[‡]Corresponding author. E-mail: xuhf@jlu.edu.cn

© 2024 Chinese Physical Society and IOP Publishing Ltd

have proved the occurrence of molecular bending during enhanced ionization.[37] The sequential versus concerted dissociation mechanism of highly charged OCS^{3+} ions produced in strong laser fields are well distinguished by employing coincidence momentum imaging, and the relative branching ratios have been obtained.[38] As a polar linear molecule, the alignment and orientation of OCS molecules have been achieved either by an all-optical method[39] or using shaped laser pulses combined with electrostatic fields.[40] Strongly asymmetric angular distributions of electrons/ions are observed for the strong-field ionization/dissociation of the oriented OCS molecules.[41–43]

Comparing extensive studies on molecular ionization and dissociation, research on the RSE process of OCS molecules induced by strong laser fields has not been addressed yet. To this end, in this study we experimentally investigate both excitation and ionization of OCS molecules in strong NIR (800 nm) and UV (400 nm) laser fields. Both parent and fragment Rydbergs or ions are observed using a time-of-flight (TOF) mass spectrometer operating under pulsed-field ionization (PFI) or normal dc electric field mode. The yields of both ions and neutral Rydbergs are investigated as a function of laser intensity and ellipticity, and the results are compared between NIR and UV strong laser fields. The mechanisms for excitation and ionization of OCS molecules in different laser fields are discussed based on the experimental results.

2. Experimental details

The experimental setup used here to investigate strong-field RSE is a conventional linear TOF mass spectrometer combined with a PFI method, which has been described in detail elsewhere.[23,44] As shown in Fig. 1, gas-phase OCS molecules are directly introduced into the reaction chamber through a 10 μm leak value with a stagnation pressure of 1 atm. The base pressure without the gas injection is 1×10^{-6} Pa and the working pressure is about 1×10^{-4} Pa. The laser system used in the study is a Ti:sapphire chirped-pulsed amplified laser (Coherent, Libra) with a central wavelength of 800 nm, a pulse duration of 50 fs, a repetition of 1 kHz and a maximum pulse energy of 4 mJ. A half-wave plate and a Glan prism are introduced into the laser beam to vary the laser intensity continuously. A quarter-wave plate is used to change the polarization of the laser. After focusing with a 25 cm plane-convex lens, the laser beam intersects with the molecular beam. The laser intensity is calibrated by comparing the measured saturation intensity of Xe atoms with that calculated by the Ammosov–Delome–Krainov model.[45]

In the PFI-mass spectrometer experiments for detection of high Rydbergs, any directly ionized ions of OCS molecules irradiated by the strong fields are pushed away from the detector by a dc electric field. After a delay time ΔT, the remaining neutral molecules and fragments in high-lying Rydberg states (M^*, M = OCS or a fragment) are then field-ionized by switching the electric field polarity in the reaction region, and the corresponding ions $(M^*)^+$ are detected by dual microchannel plates at the end of the flight tube. The flight time of $(M^*)^+$ is measured as a function of the ΔT value and exhibits an excellent linear relationship, indicating that the signal is generated by PFI of the highly excited neutral Rydbergs. In our experimental setup, the neutral Rydberg states with principal numbers $20 < n < 30$ are detected, estimated by a saddle-point model of static field ionization [$F = 1/(9n^4)$, where F is the electric field]. A digital oscilloscope (National Instruments, PXIe-5160) connected to a PC is used to record and analyze mass-resolved signals of ions and Rydbergs. All experimental data are normally averaged over 10^4 laser shots.

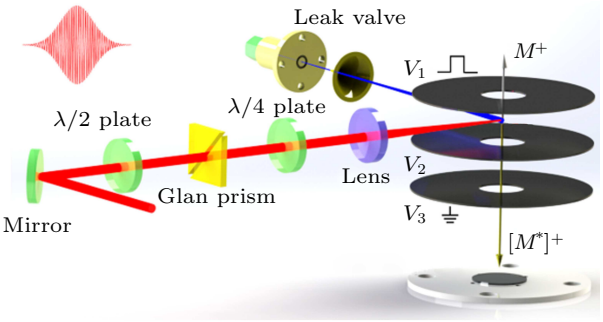


Fig. 1. Schematic diagram of the experimental setup of a linear TOF mass spectrometer combined with PFI.

3. Results and discussion

3.1. Mass spectrum of ionization/excitation of OCS

We studied ionization/excitation of OCS molecules in strong femtosecond laser fields with a TOF mass spectrometer. Typical mass spectra for strong-field ionization and RSE are shown in Figs. 2(a) and 2(b), recorded after the molecules were irradiated by linearly polarized 800 nm and 400 nm laser pulses, respectively. For strong-field ionization, singly and doubly charged parent ions (OCS^+ and OCS^{2+}) as well as various fragment ions in different charge states, including diatomic molecular fragments (OC^+) and atomic fragments ($S^{(1\sim4)+}$, $O^{(1\sim3)+}$, $C^{(1\sim3)+}$), are observed. One can see that the relative intensities of multicharged atomic ions are much stronger in 800 nm laser fields than those in 400 nm laser fields, indicating suppressed Coulomb explosion in the latter case, as also indicated in previous studies.[46] For RSE, the flight time of each $(M^*)^+$ has been subtracted by the delay time ΔT in the mass spectra in order to directly compare with the corresponding ion M^+ from strong-field ionization. The voltage in the reaction region for PFI is the same as that for direct ionization to ensure an identical detection efficiency for M^+ and $(M^*)^+$. In either 800 nm or 400 nm laser fields with an intensity of 3×10^{14} W·cm^{-2}, the parent OCS^* Rydberg is

clearly observed. This is the first experimental evidence that polyatomic molecules can survive strong laser fields in neutral high-Rydberg states. In addition, fragment Rydbergs, including atomic (C^*, O^*, S^*) and diatomic molecular (OC^*) fragments, are also observed in both laser fields. Compared with the parent OCS^* Rydberg, the fragment Rydbergs show broad peaks in the PFI mass spectra, indicating non-negligible kinetic energy releases from dissociative ionization or Coulomb explosion. To shed some light on the mechanisms of strong-field RSE and ionization of OCS, we record yields of both M^* and M^+ upon varying the laser intensity and ellipticity, as we will discuss in the following sections.

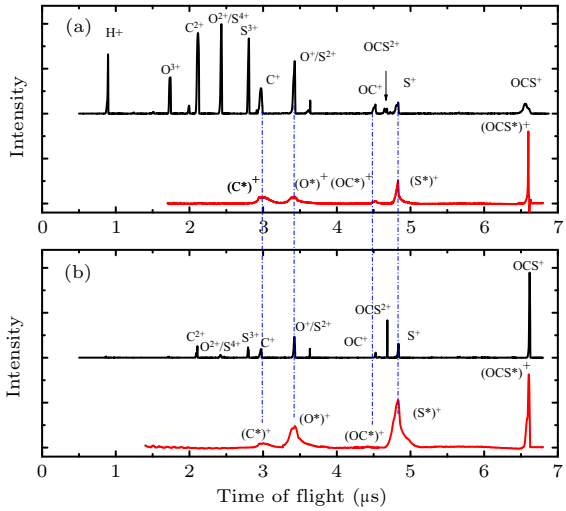


Fig. 2. TOF mass spectra of OCS obtained by direct ionization (black, upper panel) and PFI (red, lower panel) in linearly polarized 800 nm (a) or 400 nm (b) laser fields. The flight time of each $(M^*)^+$ has been subtracted by the delay time ΔT in the mass spectra. The laser intensity is kept at 3×10^{14} W·cm^{-2}.

3.2. Ionization/dissociation in NIR and UV laser fields

In Fig. 3, we show the yields of parent and fragment ions as a function of laser intensity and ellipticity in NIR (Figs. 3(a) and 3(c)) and UV (Figs. 3(b) and 3(d)) laser fields, respectively. The parent OCS^+ yields gradually increase and become saturated at 7.0×10^{13} W·cm^{-2} in the 800 nm laser fields (Fig. 3(a)), while the ionization yields keep increasing in the 400 nm laser fields in the same laser intensity region (Fig. 3(b)). The Keldysh adiabatic parameter γ[47] can be used to qualitatively distinguish the mechanisms of strong-field ionization, i.e., multiphoton ionization (MPI)[48] and tunneling ionization (TI), $\gamma=\sqrt{I_p/(2U_p)}$, where I_p represents the ionization potential of the target ($I_p=11.18$ eV for OCS) and $U_p=e^2E^2/(4m\omega^2)$ represents the ponderomotive potential in strong laser fields. If $\gamma>1$, ionization is in the MPI regime; while for $\gamma<1$ TI would be dominant in strong-field ionization. The Keldysh parameter γ is calculated and shown in the upper x-axis in Fig. 3. One would expect MPI to be the dominant ionization mechanism in 400 nm laser fields, while TI would play a more important role in the ionization of OCS molecules in 800 nm laser fields.

Doubly charged parent ions are observed in strong-field ionization of OCS in both laser fields. The intensity-dependent yields of OCS^{2+} in both linearly polarized (LP) and circularly polarized (CP) laser fields are shown in Figs. 3(a) and 3(b). In 800 nm LP laser fields a clear 'knee' structure is identified at 6.0×10^{13} W·cm^{-2} (as indicated by an arrow in Fig. 3(a)), which is a signature of the strong-field NSDI process. The suppression of the OCS^{2+} yields in CP laser fields, as well as the strong dependence on laser ellipticity at 4.0×10^{13} W·cm^{-2}, as shown in the inset of Fig. 3(a), further demonstrates the NSDI mechanism in strong-field double ionization in NIR laser fields. Since NSDI is induced by the recollision of tunneling electrons with the ionic core, its probability is greatly diminished in an elliptically polarized laser field due to the additional drift velocity of the electrons that prevents their return.[49,50] As the laser intensity increases, sequential double ionization (SDI) becomes dominant for producing OCS^{2+} ions, thus less dependence on ellipticity is observed at 1.5×10^{14} W·cm^{-2} (see the red dots in the inset of Fig. 3(a)) compared with the results in the NSDI region. These results are similar to those of double ionization of CS_2 molecules in strong 800 nm laser fields,[51,52] showing evidence of NSDI of tri-atomic molecules induced by the laser-driven electron recollision process. On the other hand, in the 400 nm laser fields, only a slight reduction in the OCS^{2+} yields is observed for the CP case compared with LP, and the yields show weak dependence on the laser ellipticity regardless of the laser intensity (Fig. 3(b)), indicating that SDI rather than NSDI dominates strong-field double ionization in the intensity region investigated here.

The intensity- and ellipticity-dependent yields of fragment ions (S^+, S^{3+}, OC^+, O^{2+}, C^+, C^{2+}, C^{3+}) are presented in Figs. 3(c) and 3(d) in NIR and UV laser fields, respectively. It can be seen from the figures that compared with singly charged fragment ions, which appear at a relatively low laser intensity, highly charged ions begin to appear at a higher laser intensity over 7.0×10^{13} W·cm^{-2} in both laser fields. This is easy to understand, since highly charged fragments are formed by dissociation/Coulomb explosion of multiply charged parent ions while singly charged fragments could be produced by dissociative ionization. In the 800 nm laser fields, all the fragment ions exhibit strong dependence on the laser ellipticity at a laser intensity of 1.5×10^{14} W·cm^{-2} (inset to Fig. 3(c)), and the dependence becomes stronger for more highly charged ions. This indicates that recollision of tunneling electrons may play an important role in the formation of fragment ions in NIR laser fields. On the other hand, the dependence on laser ellipticity is much weaker for each fragment ion produced in the 400 nm laser fields (inset in Fig. 3(d)), especially for the singly charged fragments ions (S^+, OC^+ and C^+), indicating they are produced via dissociative ionization of OCS with multi-photon absorption.

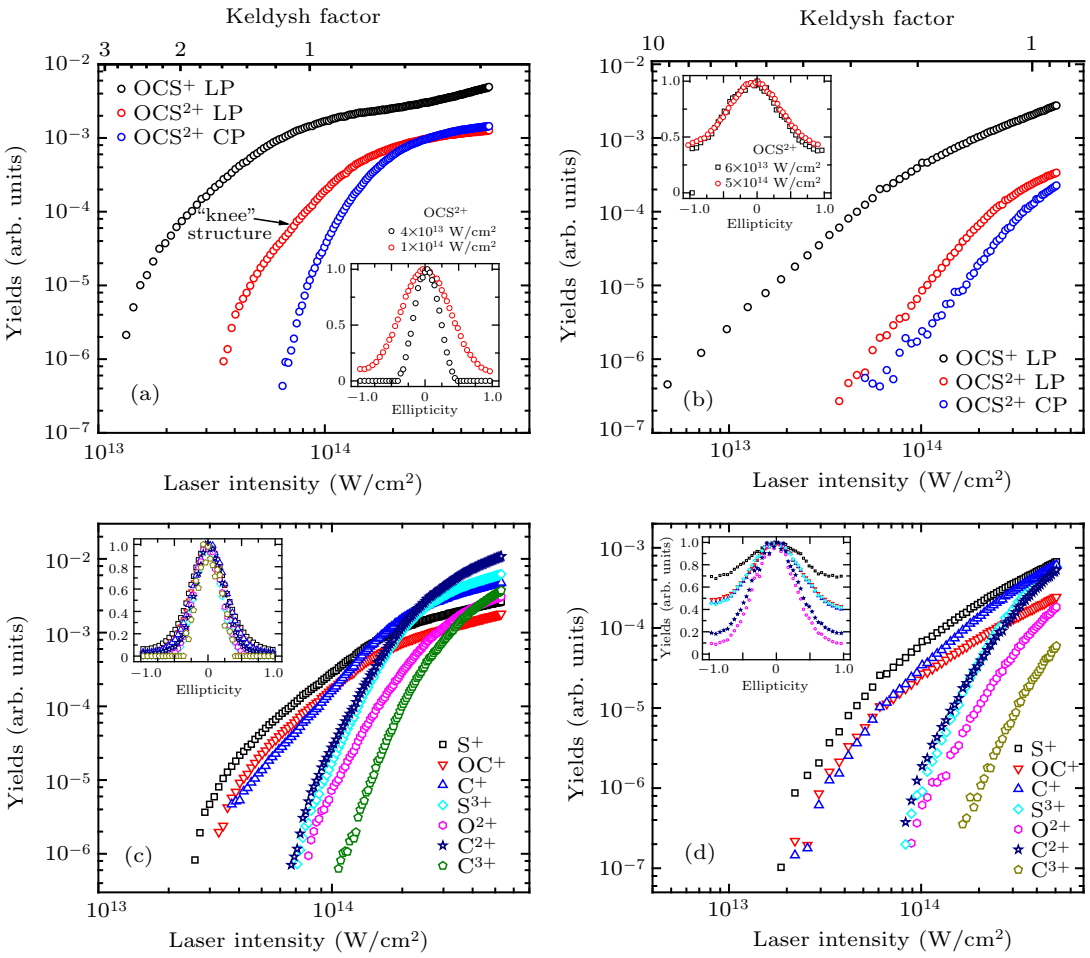


Fig. 3. The yield dependence of parent ions (OCS^+ and OCS^{2+}) on laser intensity in 800 nm (a) or 400 nm (b) laser fields with different polarizations. The yield dependence of OCS^{2+} on laser ellipticity with different laser intensities is shown in the insets of (a) and (b). The yield dependence of fragment ions on laser intensity in 800 nm (c) and 400 nm (d) laser fields. The yield dependence of fragment ions on laser ellipticity at 1.5 $\times 10^{14}$ W·cm^{-2} is shown in the insets of (c) and (d).

4. Strong-field RSE of OCS molecules

In this section we will discuss the strong-field RSE of OCS in NIR and UV laser fields. The intensity-dependent yields of parent and fragment Rydbergs are shown in Figs. 4(a) and 4(b) for strong 800 nm and 400 nm laser fields, respectively. Distinctly different behaviors in different laser fields are observed, indicating different mechanisms for the strong-field RSE process. In NIR laser fields, the parent RSE (OCS^*) is observed over the whole intensity range investigated in the study, and the yields increase as the laser intensity increases and gradually becomes saturated; the results for this are similar to those for strong-field single ionization. While the excited sulfur atoms S^* appear at a low laser intensity as the parent OCS^*, other fragment RSE can only be observed with laser intensities higher than 8×10^{13} W·cm^{-2} with much smaller yields than S^*. On the other hand, weak parent OCS^* are observed in UV laser fields until the laser intensity reaches 1.8×10^{14} W·cm^{-2}, while all the excited atom fragments (C^*, O^* and S^*) are dominant and appear at a low laser intensity of 2×10^{13} W·cm^{-2}. It is worth mentioning that although the tendencies of the intensity-dependent yields of C^* and O^* are similar, that of S^* is apparently different, indicating the different mechanisms for fragment RSE.

In Figs. 5(a) and 5(b) we show the dependence of neutral Rydberg M^* yields on laser ellipticity in strong NIR and UV laser fields, respectively. It is well known that there are two possible mechanisms for atomic RSE induced by strong laser fields, i.e., frustrated tunneling ionization (FTI)[10] and multi-photon resonance excitation.[18] For FTI, the RSE yields will be strongly depressed in elliptical polarized laser fields owing to the decline in low-energy photo-electrons that could be captured into Rydberg states by the Coulomb potential.[44] However, a weak ellipticity dependence is expected for the RSE process induced by multi-photon resonance excitation.[53,54] One can see from Fig. 5 that much stronger dependence on laser ellipticity is observed for M^* in 800 nm laser fields (Fig. 5(a)) compared with the results in 400 nm laser fields (Fig. 5(b)). Our study indicates that for OCS molecules both neutral parent and fragment Rydbergs could be produced by FTI or recapture of the tunneling electrons in strong NIR laser fields, while multi-photon resonance excitation plays a more important role in RSE in UV laser fields.

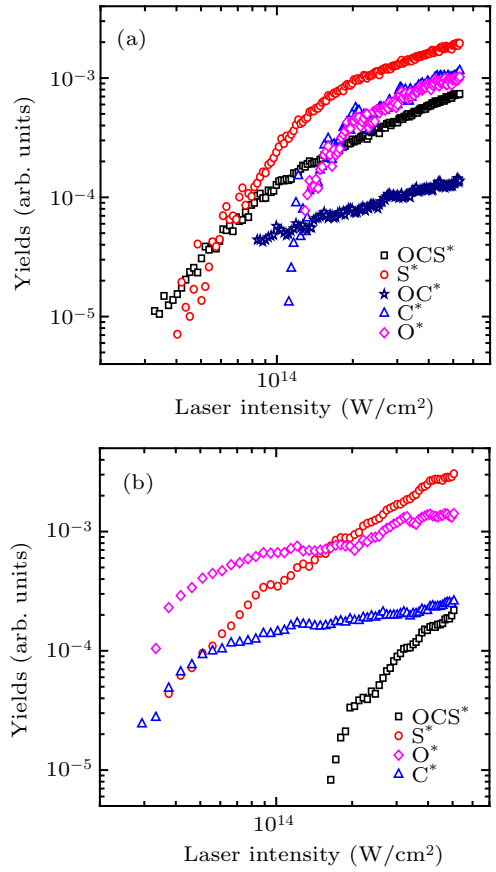


Fig. 4. Dependence of the parent and fragment RSE yields of OCS on the laser intensity of linearly polarized 800 nm (a) and 400 nm (b) laser fields.

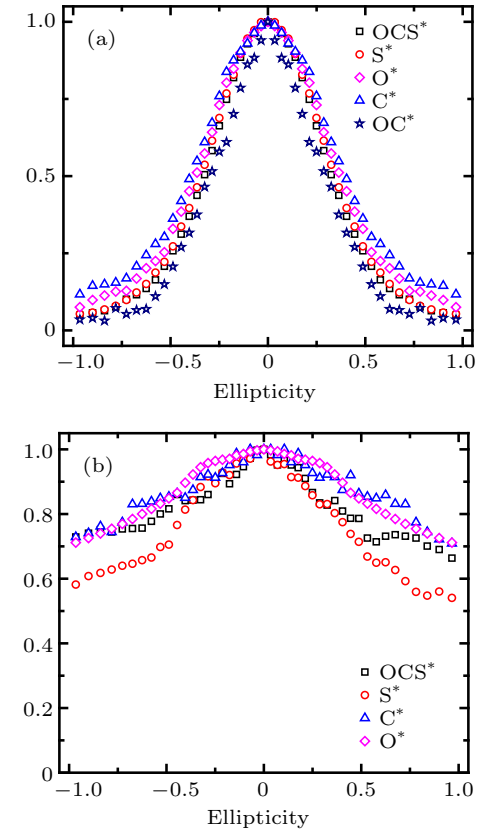


Fig. 5. Dependence of the parent and fragment RSE yields of OCS on the laser ellipticity of the 800 nm (a) and 400 nm (b) laser fields. The laser intensity is kept at 3×10^{14} W·cm^{-2}.

Table 1. Appearance laser intensity (I_{app}, W·cm^{-2}) obtained from the intensity-dependent curves in Fig. 4, the full width at half maximum (FWHM) and the yield ratio between CP and LP laser fields $R_{CP/LP}$ obtained from the ellipticity-dependent curves in Fig. 5 for parent and fragment Rydbergs in strong 800 nm and 400 nm laser fields.

		OCS*	OC*	S*	O*	C*
I_{app} (W·cm^{-2})	800 nm	3×10^{13}	8×10^{13}	4×10^{13}	1×10^{14}	1×10^{14}
	400 nm	1.8×10^{14}	–	3×10^{13}	3×10^{13}	3×10^{13}
FWHM	800 nm	0.64	0.61	0.66	0.66	0.7
	400 nm	0.67	–	0.84	1.05	1.08
$R_{CP/LP}$	800 nm	0.03	0.03	0.05	0.07	0.12
	400 nm	0.73	–	0.58	0.7	0.7

In Table 1, we summarize the appearance laser intensity and yield ratio between CP and LP laser fields of parent and fragment Rydbergs in 800 nm and 400 nm laser fields. As mentioned above, in strong NIR laser fields different fragment M^*s, which have a similar FWHM of their ellipticity dependence curves, exhibit distinctly different intensity-dependent behaviors, indicating they are produced by recapturing the tunneling electron via different channels. It is noted that the fragment S^* is visible at a low laser intensity of 4×10^{13} W·cm^{-2}, which is close to the intensity at which the S^+ or OCS^{2+} ions appear (see Fig. 3). In addition, the ellipticity-dependent curves of S^* and S^+ are similar. These observations strongly indicate that S^* is attributed to the recapture of low-energy photo-electrons of corresponding S^+ ions, most probably via Coulomb explosion of doubly charged OCS^{2+} ions (i.e., $OCS^{2+}\rightarrow S^+ + OC^+$). Actually, recent studies indicate that a third of the OCS^{2+} ions produced in strong laser fields are unstable and finally dissociate to fragment ions.[32] The fact that the yields of S^* are much higher than those of OC^* strongly indicates that the electrons are recaptured by the atomic fragment ions S^+ rather than by the diatomic fragment ions OC^+ from Coulomb explosion of OCS^{2+}. This could be understood by the orientation-dependent ionization of OCS molecules in strong laser fields. That is, the OCS molecules prefer to be ionized when the electric field points to the S atom along the molecular axis;[55] thus the ionized electrons would be ejected in the same direction as S^+ ions, leading to a higher recapture probability by S^+ to produce S^*. Concerning the other two fragments C^* and O^*, the intensity-dependence curves are apparently different from those of the corresponding ions C^+ and O^+. Taking C^* as an example, it is only observed when the laser intensity is higher than 1×10^{14} W·cm^{-2}, while C^+appears at a relatively low laser intensity of 3×10^{13} W·cm^{-2}. This indicates that the C^+ ions produced at a low laser intensity make no contribution to the formation of C^*. We expect that C^* and O^* could be formed by the recapture of low-energy photo-electrons during Coulomb explosion of highly charged parent ions, OCS^{n+} ($n>2$), which would be more pronounced in the higher laser intensity region. The similar dependence of fragments C^* and O^* on laser intensity of NIR laser fields indicates that they are

produced in the same Coulomb explosion channel, and C^+ and O^+ ions have a similar electron capture capability.

In strong UV laser fields, however, all the atomic fragment Rydbergs (S^*, C^* and O^*) can be observed even at a low intensity of 3×10^{13} W·cm^{-2} (Fig. 4(b) and Table 1). The FWHM of ellipticity dependence of these Rydberg M^*s in UV laser fields is clearly larger than that in NIR laser fields. In particular, the yield ratio between CP and LP laser fields of Rydberg M^*s in UV laser fields is in the range of 0.6–0.7 (Table 1), indicating much less suppression of RSE in CP laser fields. The weak ellipticity dependence of M^* shown in Fig. 5(b) indicates that the dominant mechanism is multi-photon resonance excitation. Generally, molecular Rydberg states excited by multi-photon resonance excitation would be embedded in high-lying valance states with a large density-of-states and would dissociate to form excited fragments. This also explains the observation that the parent OCS^* is much weaker than the fragments in 400 nm laser fields, and can be observed only with a laser intensity higher than 1.8×10^{14} W·cm^{-2} (Fig. 4(b)). The yields of C^* and O^* become saturated at a low intensity of 6×10^{13} W·cm^{-2} (Fig. 4(b)), further proving that C^* and O^* fragments are produced by dissociation of parent OCS^*. The yield of O^* is several times higher than that of C^*, a result which is different from that in 800 nm laser fields. The OC^* yield in 400 nm laser fields is too small to be observed over the whole intensity range investigated in this study. These observations indicate that the relative yields of fragment Rydberg atoms in 400 nm laser fields are not determined by the ionic electron capture capability but rather by the branching ratio of dissociation channels. Nevertheless, we cannot completely exclude FTI or the recapture mechanism in strong UV laser fields, especially with increasing laser intensity. Note that the behavior of the intensity-dependent curve of S^* is quite different from those of C^* and O^* in 400 nm laser fields, as shown in Fig. 4(b). Since the OCS^{2+} ions appear at laser intensities as low as 2×10^{13} W·cm^{-2} (Fig. 3(b)), the recapture of electrons by S^+ to form S^*, as discussed above for NIR laser fields, could also play a role in UV laser fields. Further channel-resolved coincidence or imaging experimental setups, combined with the PFI method, would be a promising approach to further reveal the underlying physics of fragment RSE of molecules in different strong laser fields.

5. Conclusion

In summary, we experimentally investigated the excitation and ionization of OCS molecules in strong NIR and UV laser fields. By measuring the yield-dependence of ions and neutral Rydbergs on laser intensity and ellipticity, the mechanism for strong field ionization and RSE in different laser fields is discussed. It is indicated that neutral Rydbergs could be produced by FTI or recapture of the tunneling electron in strong NIR laser fields, while multi-photon resonance excitation plays a more important role in RSE in UV laser fields. In addition, our results indicate that fragment Rydbergs are formed by corresponding ions that are produced in Coulomb explosion of highly charged parent ions in 800 nm laser fields, while dissociation of parent Rydberg molecules is the main mechanism for fragment Rydbergs in 400 nm laser fields. Our results shed some light on the RSE of OCS molecules in different laser fields, and should stimulate further research on strong-field RSE of polyatomic molecules.

Acknowledgements

Project supported by the National Key Program for S&T Research and Development (Grant No. 2019YFA0307700) and the National Natural Science Foundation of China (Grant Nos. 12174148, 11874179, 12074144, and 12074146).

References

[1] Wolter B, Pullen M G, Baudisch M, Sclafani M, Hemmer M, Senftleben A, Schröter C D, Ullrich J, Moshammer R and Biegert J 2015 *Phys. Rev. X* **5** 21034
[2] Vozzi C, Negro M and Stagira S 2012 *J. Mod. Optic* **59** 1283
[3] Protopapas M, Keitel C H and Knight P L 1997 *Rep. Prog. Phys.* **60** 389
[4] Tang J, Zhang G, He Y, Li M, Ding X and Yao J 2020 *Chin. Phys. Lett.* **37** 24201
[5] Fittinghofr D N, Bolton P R, Chang B and Kulander K C 1992 *Phys. Rev. Lett.* **69** 2642
[6] Auguste T, Monot P, Lompé L A, Mainfray G and Manus C 1992 *J. Phys. B: At. Mol. Opt. Phys.* **25** 4181
[7] Quan W, Lai X, Chen Y, Wang C, Hu Z, Liu X, Hao X, Chen J, Hasović E, Busuladžić M, Becker W and Milošević D B 2013 *Phys. Rev. A* **88** 21401
[8] Corkum P B, Burnett N H and Brunel F 1989 *Phys. Rev. Lett.* **62** 1259
[9] Ferray M, L'Huillier A, Li XF, Lomprk LA, Mainfray G and Manus C 1988 *J. Phys. B: At. Mol. Opt. Phys.* **21** L31
[10] Nubbemeyer T, Gorling K, Saenz A, Eichmann U and Sandner A W 2008 *Phys. Rev. Lett.* **101** 233001
[11] Wang B B, Li X F, Fu P M, Chen J and Liu J 2006 *Chin. Phys. Lett.* **23** 2729
[12] Eichmann U, Nubbemeyer T, Rottke H and Sandner W 2009 *Nature* **461** 1261
[13] Yun H, Mun J H, Hwang S I, Park S B, Ivanov I A, Nam C H and Kim K T 2018 *Nat. Photon.* **12** 620
[14] Liu M, Xu S, Hu S, Becker W, Quan W, Liu X and Chen J 2021 *Optica* **8** 765
[15] Shvetsov-Shilovskia N I, Goreslavskia S P, Popruzhenkoa S V and Beckerb W 2009 *Laser Phys.* **19** 1550
[16] Sun T, Zhao L, Liu Y A, Guo J, Lv H and Xu H 2023 *Phys. Rev. A* **108** 13120
[17] Popov A M, Tikhonova O V and Volkova E A 2014 *J. Phys. B: At. Mol. Opt. Phys.* **47** 204012
[18] Popov A M, Tikhonova O V and Volkova E A 2010 *Laser Phys.* **20** 1028
[19] Zimmermann H, Patchkovskii S, Ivanov M and Eichmann U 2017 *Phys. Rev. Lett.* **118** 13003
[20] Li Q, Tong X, Morishita T, Jin C, Wei H and Lin C D 2014 *J. Phys. B: At. Mol. Opt. Phys.* **47** 204019
[21] Shu Z, Liu M, Hu S and Chen J 2020 *Opt. Express* **28** 11165
[22] Hu S, Hao X, Lv H, Liu M, Yang T, Xu H, Jin M, Ding D, Li Q, Li W, Becker W and Chen J 2019 *Opt. Express* **27** 31629
[23] Lv H, Zuo W L, Zhao L, Xu H F, Jin M X, Ding D J, Hu S L and Chen J 2016 *Phys. Rev. A* **93** 33415
[24] Emmanouilidou A, Lazarou C, Staudte A and Eichmann U 2012 *Phys. Rev. A* **85** 11402

[25] McKenna J, Zeng S, Hua J J, Sayler A M, Zohrabi M, Johnson N G, Gaire B, Carnes K D, Esry B D and Ben-Itzhak I 2011 *Phys. Rev. A* **84** 43425

[26] Nubbemeyer T, Eichmann U and Sandner W 2009 *J. Phys. B: At. Mol. Opt. Phys.* **42** 134010

[27] Zhang W, Lu P, Gong X, Li H, Ji Q, Lin K, Ma J, Li H, Sun F, Qiang J, Chen F, Tong J and Wu J 2020 *Phys. Rev. A* **101** 033401

[28] von Veltheim A, Manschwetus B, Quan W, Borchers B, Steinmeyer G, Rottke H and Sandner W 2013 *Phys. Rev. Lett.* **110** 23001

[29] Xie X, Wu C, Liu H, Li M, Deng Y, Liu Y, Gong Q and Wu C 2013 *Phys. Rev. A* **88** 65401

[30] McKenna J, Sayler A M, Gaire B, Kling N G, Esry B D, Carnes K D and Ben-Itzhak I 2012 *New J. Phys.* **14** 103029

[31] Hikosaka Y 2023 *J. Chem. Phys.* **158** 214306

[32] Jarraya M, Wallner M, Ben Yaghlane S, Olsson E, Ideböhn V, Squibb R J, Palaudoux J, Nyman G, Al-Mogren M M, Eland J H D, Feifel R and Hochlaf M 2023 *Phys. Chem. Chem. Phys.* **25** 19435

[33] Ramadhan A, Wales B, Karimi R, Gauthier I, MacDonald M, Zuin L and Sanderson J 2016 *J. Phys. B: At. Mol. Opt. Phys.* **49** 215602

[34] Wang B, Han J, Zhu X, Wei L, Ren B, Zhang Y, Yu W, Yan S, Ma X, Zou Y, Chen L and Wei B 2021 *Phys. Rev. A* **103** 042810

[35] Sharma D, Bapat B, Bhatt P and Safvan C P 2020 *J. Phys. B: At. Mol. Opt. Phys.* **53** 155202

[36] Ma P, Wang C, Luo S, Li X, Hu W, Yu J, Yu X, Tian X, Qu Z and Ding D 2019 *Phys. Rev. A* **99** 023423

[37] Wales B, Bisson É, Karimi R, Beaulieu S, Ramadhan A, Giguère M, Long Z, Liu W, Kieffer J, Légaré F and Sanderson J 2014 *J. Electron. Spectrosc.* **195** 332

[38] Rajput J, Severt T, Berry B, Jochim B, Feizollah P, Kaderiya B, Zohrabi M, Ablikim U, Ziaee F, Raju P K, Rolles D, Rudenko A, Carnes K D, Esry B D and Ben-Itzhak I 2018 *Phys. Rev. Lett.* **120** 103001

[39] Oda K, Hita M, Minemoto S and Sakai H 2010 *Phys. Rev. Lett.* **104** 213901

[40] Goban A, Minemoto S and Sakai H 2008 *Phys. Rev. Lett.* **101** 13001

[41] Sakemi Y, Minemoto S and Sakai H 2017 *Phys. Rev. A* **96** 011401

[42] Hansen J L, Holmegaard L, Nielsen J H, Stapelfeldt H, Dimitrovski D and Madsen L B 2012 *J. Phys. B: At. Mol. Opt. Phys.* **45** 15101

[43] Holmegaard L, Hansen JL, Kalhøj L, Louise Kragh S, Stapelfeldt H, Filsinger F, Küpper J, Meijer G, Dimitrovski D, Abu-samha M, Martiny C P J and Bojer Madsen L 2010 *Nat. Phys.* **6** 428

[44] Zhao L, Dong J, Lv H, Yang T, Lian Y, Jin M, Xu H, Ding D, Hu S and Chen J 2016 *Phys. Rev. A* **94** 053403

[45] Ammosov M V, Delone N B and Krainov V P 1986 *Soviet Physics Jetp* **64** 1191

[46] Zuo W, Lv H, Zhao L, Zhang Q and Xu H 2015 *Int. J. Mass Spectrom* **392** 80

[47] Popov V S 2004 *Phys.-Usp.* **47** 855

[48] Guo K, Li M, Liang J, Cao C, Zhou Y and Lu P 2023 *Chin. Phys. B* **32** 23201

[49] Corkum P B 1993 *Phys. Rev. Lett.* **71** 1994

[50] Corkum P B 2011 *Phys. Today* **64** 36

[51] Xu Q, Ben S, Sun Y, Xu H, Liu X, Lv H and Guo J 2020 *Chem Phys. Lett.* **747** 137326

[52] Zuo W, Ben S, Lv H, Zhao L, Guo J, Liu X, Xu H, Jin M and Ding D 2016 *Phys. Rev. A* **93** 53402

[53] Yang T X, Lian Y, Wang R, Zhang S W, He L H, Lv H and Xu H F 2017 *J. at Mol. Sci.* **8** 49

[54] Lv H, Zhang J F, Zuo W L, Xv H F, Jing M X and Ding D J 2015 *Chin. Phys. B* **24** 063303

[55] Dimitrovski D, Abu-samha M and Madsen L B 2011 *Phys. Rev. A* **83** 23405